

Fast Two-Dimensional Atomic Norm Minimization in Spectrum Estimation and Denoising

Jian Pan *Student Member, IEEE*, Jun Tang, *Member, IEEE*, and Yong Niu, *Member, IEEE*

Abstract—Motivated by recent work on two dimensional (2D) harmonic component recovery via atomic norm minimization (ANM), a fast 2D direction of arrival (DOA) off-grid estimation based on ANM method was proposed. By introducing a matrix atomic norm the 2D DOA estimation problem is turned into matrix atomic norm minimization (MANM) problem. Since the 2D-ANM gridless DOA estimation is processed by vectorizing the 2D into 1D estimation and solved via semi-definite programming (SDP), which is with high computational cost in 2D processing when the number of antennas increases to large size. In order to overcome this difficulty, a detail formulation of MANM problem via SDP method is offered in this paper, the MANM method converts the original $MN + 1$ dimensions problem into a $M + N$ dimensions SDP problem and greatly reduces the computational complexity. In this paper we study the problem of 2D line spectrally-sparse signal recovery from partial noiseless observations and full noisy observations, both of which can be solved efficiently via MANM method and obtain high accuracy estimation of the true 2D angles. We give a sufficient condition of the optimality condition of the proposed method and prove an up bound of the expected error rate for denoising. Finally, numerical simulations are conducted to show the efficiency and performance of the proposed method, with comparisons against several existed sparse methods.

Index Terms—Sparse recovery, matrix atomic norm, 2-Deminsion, signal denoise.

I. INTRODUCTION

Estimating the frequencies of a superposition of complex harmonic 2D signals arises in many applications, including the direction of arrival estimation in radar target tracking and location [1] [2], multiple-input multiple-output (MIMO) antennas communication channel estimation [3] [4], and super-resolution imaging through a Fourier imaging system [5]. All of these applications can be attributed to 2D DOA estimation problem.

Conventional 2D DOA estimation methods are often based on Subspace theory methods such as 2D unitary ESPRIT [6], 2D MUSIC [7], and the Matrix Enhancement Matrix Pencil (MEMPE) method [8], etc. However, most of these methods rely on the covariance of sampled observation, which requires that the number of independent observations should be larger than the antenna numbers. what's more, they may fail for coherent sources [9]. Since last decade, researchers have put forward super resolution DOA estimation methods based on compressed sensing (CS) [10] theory, which exploits

source sparsity for frequency or angular estimation [11] [12] and enables DOA estimation even from a single snapshot of measurements, regardless of source correlation. The CS based DOA estimation methods are implemented via discretizing the 2D possible angle scope with grid points and then recovering the true location by sparse recovery methods such as basis pursuit (BP) [13], least absolute shrinkage and selection operation (LASSO) [14], orthogonal matching pursuit (OMP) [15] and so on. These sparse methods result in fine estimation performance if the true angle location satisfies the pairwise isometry property (PIP) [16] and the grids are dense enough. However, researchers have found that if the observed signal contains off-grid harmonic components it may result in considerable performance decreasing via conventional sparse approximation algorithms over the discrete basis, which has been pointed out in [17] [18] [19]. Therefore, it is necessary to design a parameter estimation method, which is not relevant to the priori basis for sparse reconstruction while still utilizing the sparsity property.

Recently, a new gridless sparse recovery method for spectral estimation is developed via atomic norm minimization (ANM) [20], which provides a structure-based optimization approach that utilizing the Vandermonde structure of the captured data in a SDP via Toeplitz matrix [21] [22]. The ANM method works well in recovering a spectrally-sparse signal from a few numbers of randomly selected samples of the complete observation data [23] [24]. However, ANM method can not be directly extended to the 2D case by vectorizing the matrix data into vector data and solving the 1D ANM optimum problem, i.e. the equivalence between the 2D atomic norm minimization in its 1D SDP form is not guaranteed, since the Vandermonde decomposition of Toeplitz matrix via Caratheodory's theorem does not hold in higher dimensions. Pioneered by Chi [25] vectorized -ANM for 2D frequency estimation has been exploited, which turns the 2D frequency estimation into a double-folds Toeplitz matrix SDP problem. This method retains the merits of the ANM approach in terms of super-resolution from single-snapshot observations, and robustness to source correlation. But its computation complexity is very high, which becomes almost intractable when the dimensions of antenna array become large.

In this paper, a new definition of ANM is formulated via introducing a new atom set based on 2D harmonic component matrix which turns the double-folds Toeplitz matrix into two Toeplitz matrices with harmonic component contained in one dimension. Accordingly, a new SDP problem is formed for the matrix ANM (MANM), which has greatly decreased the optimum problem's size and remarkably improved computational

Jian Pan, and Jun Tang are with the Department of Electronic Engineering, Tsinghua University, Beijing, 100084, China (email: jianlonger@126.com, tang_ee@mail.tsinghua.edu.cn). Yong Niu is with State Key Laboratory of Rail Traffic Control and Safety, Beijing Jiaotong University, Beijing 100044, China (E-mails: niuy11@163.com). This work was supported in part by National Natural Science Foundation of China under Grant 61171120.

efficiency. The run time of MANM method is several orders of magnitude lower than of VANM method, while all other advantages of ANM are reserved such as high accuracy, high resolution and a small number of observation requirements. Theoretic formulations of our method are given in both proofs and simulations to validate the proposed MANM method.

The rest of this paper is organized as follows. In Section II, system model and problem, related literature and introduction to MANM are described. In Section III, the proposed matrix atomic norm minimization algorithm for full data recovery from partial noiseless observations and data denoise from full noisy observations via SDP are formulated, and their performance guarantee and proof are deferred to the Appendix B and Appendix C. In Section IV, Numerical simulations are conducted to test the efficiency and performance of proposed algorithm. Finally, this paper is concluded in Section V.

Notations: Throughout the paper, matrices are denoted by bold capital letters, and vectors by bold lowercase letters. $(\cdot)^T, (\cdot)^*, (\cdot)^H$ denote the transpose, conjugate and conjugate transpose, respectively. $\|\cdot\|$ denotes the Euclidean norm and $\|\cdot\|_F$ denotes the Frobenius norm of matrix. $\text{Tr}(\cdot)$ denotes the trace of a matrix, and $\langle \mathbf{A}, \mathbf{B} \rangle \triangleq \text{Tr}(\mathbf{B}^H \mathbf{A})$ stands for the inner product of matrix \mathbf{A} and \mathbf{B} . $\langle \mathbf{A}, \mathbf{B} \rangle_{\mathbb{R}} \triangleq \text{Re}(\langle \mathbf{A}, \mathbf{B} \rangle)$ represent the real part of the inner product. \otimes denotes the Kronecker product. \mathbb{R} and \mathbb{C} denotes the sets of all real numbers and complex numbers, respectively. $\mathbb{P}(\cdot)$ denote the probability of incident (\cdot) and $\mathbb{E}(\cdot)$ denotes the expectation of the argument.

II. PROBLEM FORMULATION AND THE DEFINITION OF ATOMIC NORM

In this section the sparse 2D-harmonic signal model is formulated via a typical example and a new kind of atomic norm is introduced to fast estimate 2D harmonic component.

A. Signal Model

Assume that there are K source signals in far-field scene with their echo impinge on an $M \times N$ Uniform Rectangle Array (URA) which contains M and N antenna elements along x -direction and y -direction. Let (θ_k, φ_k) be the azimuth angle and elevation angle of the k -th source signal as is shown in Fig. 1.

As for the k -th source signal, let (r_x, r_y, r_z) denotes the

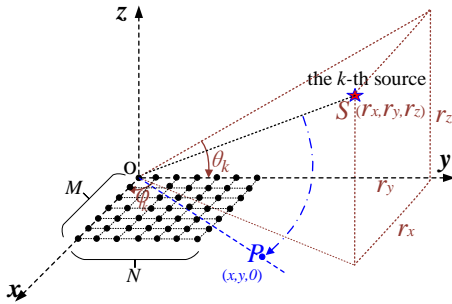


Fig. 1. Source signal in far field for a $M \times N$ Uniform Rectangle Array (URA)

location of the k -th source signal in 3 dimension coordinates,

then for a point P locate at $(x, y, 0)$ in $x - O - y$ plane, the path difference with respect to the antenna element at origin O (coordinate $(0, 0, 0)$) is

$$\Delta d = \frac{r_x \cdot x + r_y \cdot y}{\sqrt{r_x^2 + r_y^2 + r_z^2}} \quad \text{s.t.} \quad \begin{cases} \tan(\theta_k) = r_x / \sqrt{r_x^2 + r_y^2} \\ \tan(\varphi_k) = r_y / r_x. \end{cases} \quad (1)$$

Let d_x, d_y denote the inter-element spacing with respect to x -direction and y -direction, if $(x, y) = (m d_x, n d_y)$ then the phase difference $\Delta \Phi$ that with respect to the antenna element at origin O is

$$\Delta \Phi = 2\pi m \cdot f_{x,k} + 2\pi n \cdot f_{y,k} \quad (2)$$

$$f_{x,k} \triangleq \frac{1}{\lambda_c} \cos \varphi_k \cos \theta_k \quad (3)$$

$$f_{y,k} \triangleq \frac{1}{\lambda_c} \sin \varphi_k \cos \theta_k \quad (4)$$

where λ_c is the wavelength of received echo.

Hence, the total received target echo data matrix without noise to this URA can be written as

$$\mathbf{X} = [x_{m,n}]_{M \times N} \quad 0 \leq m \leq M-1, 0 \leq n \leq N-1$$

$$x_{m,n} = \sum_{k=0}^K \frac{1}{\sqrt{MN}} s_k^* \cdot e^{-j2\pi \cdot (m f_{x,k} + n f_{y,k})} \quad (5)$$

where, $s_k^* \in \mathbb{C}$ denotes the echo strength of the k -th source signal, $(f_{x,k}, f_{y,k})$ are normalized spatial frequency factors that decided by (θ_k, φ_k) via (3) and (4). It is easy to see that (5) can be rewritten in a brief form as

$$\mathbf{X} = \sum_{k=0}^K s_k^* \cdot \mathbf{a}_x(f_{x,k}) \cdot \mathbf{a}_y^T(f_{y,k}) = \mathbf{A}_x \cdot \mathbf{S} \cdot \mathbf{A}_y^T \quad (6)$$

where

$$\mathbf{a}_x(f_{x,k}) \triangleq [1, e^{-j2\pi \cdot f_{x,k}}, \dots, e^{-j2\pi \cdot (M-1) f_{x,k}}]^T \quad (7)$$

$$\mathbf{a}_y(f_{y,k}) \triangleq [1, e^{-j2\pi \cdot f_{y,k}}, \dots, e^{-j2\pi \cdot (N-1) f_{y,k}}]^T \quad (8)$$

$$\mathbf{S} \triangleq \text{diag}(\mathbf{s}^*), \quad \mathbf{s}^* = [s_1^*, s_2^*, \dots, s_K^*]^T \quad (9)$$

$$\mathbf{A}_x \triangleq [\mathbf{a}_x(f_{x,1}), \mathbf{a}_x(f_{x,2}), \dots, \mathbf{a}_x(f_{x,K})] \quad (10)$$

$$\mathbf{A}_y \triangleq [\mathbf{a}_y(f_{y,1}), \mathbf{a}_y(f_{y,2}), \dots, \mathbf{a}_y(f_{y,K})]. \quad (11)$$

The goal of 2D DOA estimation for URA is identical to recovery $\{(f_{x,k}, f_{y,k})\}_{k=1}^K$ from its observation \mathbf{X} in (5), since $\{(\theta_k, \varphi_k)\}_{k=1}^K$ can be obtained by solving (3) and (4). without loss of generality, we turn to estimate $\{(f_{x,k}, f_{y,k})\}_{k=1}^K$ instead.

B. Vectorial Atomic Norm for 2D DOA model

In [25] [26] the Vectorial Atomic Norm is defined via vectorized the data matrix to get an large dimension atom set. Let $\mathbf{x} = \text{vec}(\mathbf{X}) \in \mathbb{C}^{MN \times MN}$ be the vectorized data matrix, then one has

$$\mathbf{x} = (\mathbf{A}_y \otimes \mathbf{A}_x) \cdot \text{vec}(\mathbf{S}) = \sum_{k=1}^K s_k^* \cdot \mathbf{a}_y(f_{y,k}) \otimes \mathbf{a}_x(f_{x,k})$$

$$= \sum_{k=1}^K \sqrt{MN} s_k^* \cdot \mathbf{c}(\mathbf{f}_k) \quad (12)$$

where

$$\mathbf{c}(\mathbf{f}_k) \triangleq \mathbf{c}(f_{x,k}, f_{y,k}) = \frac{1}{\sqrt{MN}} \mathbf{a}_X(f_{x,k}) \otimes \mathbf{a}_Y(f_{y,k}). \quad (13)$$

The atom set \mathcal{A}_v is defined as the collection of all normalized 2-D complex harmonic:

$$\begin{aligned} \mathcal{A}_v &= \{ \mathbf{c}(\mathbf{f}) \mid \mathbf{c}(\mathbf{f}) \in \mathbb{C}^{MN}, \mathbf{f} \in [0, 1] \times [0, 1] \} \\ \mathbf{c}(\mathbf{f}) &\triangleq \mathbf{c}(f_x, f_y) = \frac{1}{\sqrt{MN}} \mathbf{a}_X(f_x) \otimes \mathbf{a}_Y(f_y) \end{aligned} \quad (14)$$

and the atomic norm of \mathbf{x} can be calculated as

$$\begin{aligned} \|\mathbf{x}\|_{\mathcal{A}_v} &= \inf \left\{ \sum_k |d_k| \mid \mathbf{x} = \sum_k d_k \mathbf{c}(\mathbf{f}_k), \mathbf{c}(\mathbf{f}_k) \in \mathcal{A}_v \right\} \\ &= \min_{\substack{\mathbf{U} \in \mathbb{C}^{M \times N} \\ v \in \mathbb{C}}} \left\{ \frac{1}{2} v + \frac{1}{2} \text{Tr}(\mathcal{T}_{2D}(\mathbf{U})) \right\} \\ &\quad \text{s.t.} \begin{bmatrix} \mathcal{T}_{2D}(\mathbf{U}) & \mathbf{x} \\ \mathbf{x}^H & v \end{bmatrix} \succeq \mathbf{0} \end{aligned} \quad (15)$$

where, $\mathbf{U} = [u_{(i,k)}]_{M \times N}$ and $\mathcal{T}_{2D}(\mathbf{U})$ is a two-fold block Hermite Toeplitz matrix which is defined as

$$\begin{aligned} \mathcal{T}_{2D}(\mathbf{U}) &= \begin{bmatrix} \mathbf{T}_1 & \mathbf{T}_2 & \dots & \mathbf{T}_M \\ \mathbf{T}_2^* & \mathbf{T}_1 & \dots & \mathbf{T}_{M-1} \\ \vdots & \vdots & \dots & \vdots \\ \mathbf{T}_M^* & \mathbf{T}_{M-1}^* & \dots & \mathbf{T}_1 \end{bmatrix}, \quad (16) \\ \mathbf{T}_l &= \begin{bmatrix} u_{(l,1)} & u_{(l,2)} & \dots & u_{(l,N)} \\ u_{(l,2)}^* & u_{(l,1)} & \dots & u_{(l,N-1)} \\ \vdots & \vdots & \dots & \vdots \\ u_{(l,N)}^* & u_{(l,N-1)}^* & \dots & u_{(l,1)} \end{bmatrix}. \end{aligned} \quad (17)$$

C. Matrix Atomic Norm for 2D DOA model

According to the signal model (6) to (11), the matrix atom set is defined as all matrices that decided by $\{(f_{x,k}, f_{y,k})\}_k$, i.e.,

$$\mathcal{A}_m \triangleq \{ \mathbf{A}_m(\mathbf{f}) \mid \mathbf{f} \in [0, 1] \times [0, 1] \} \quad (18)$$

where

$$\mathbf{A}_m(\mathbf{f}_k) = \mathbf{a}_X(f_{x,k}) \cdot \mathbf{a}_Y^T(f_{y,k}) \quad (f_{x,k}, f_{y,k}) \in [0, 1] \times [0, 1]$$

and the atomic norm of \mathbf{X} can be calculated as

$$\|\mathbf{X}\|_{\mathcal{A}_m} = \inf \left\{ \sum_k |s_k| \mid \mathbf{X} = \sum_k s_k \mathbf{A}_m(\mathbf{f}_k), \mathbf{A}_m(\mathbf{f}) \in \mathcal{A}_m \right\}. \quad (19)$$

which is the gauge function associated with the convex hull of \mathcal{A}_m . Encouragingly, the matrix atomic norm satisfies the following equivalent SDP form, which can be computed efficiently. The proof can be found in Appendix A.

Theorem 1 *If $\mathbf{X} \in \mathbb{C}^{M \times N}$, then the matrix atom norm $\|\mathbf{X}\|_{\mathcal{A}_m}$ can be rewritten as*

$$\begin{aligned} \|\mathbf{X}\|_{\mathcal{A}_m} &= \inf_{(\mathbf{u}, \mathbf{v}) \in \mathbb{C}^M \times \mathbb{C}^N} \text{Tr} \left(\frac{1}{2M} \mathcal{T}(\mathbf{u}) + \frac{1}{2N} \mathcal{T}(\mathbf{v}) \right) \\ &\quad \text{s.t.} \begin{bmatrix} \mathcal{T}(\mathbf{u}) & \mathbf{X} \\ \mathbf{X}^H & \mathcal{T}(\mathbf{v}) \end{bmatrix} \succeq \mathbf{0} \end{aligned} \quad (20)$$

where, $\mathcal{T}(\mathbf{u})$ and $\mathcal{T}(\mathbf{v})$ are Hermite Toeplitz matrices with vector \mathbf{u} and \mathbf{v} as their first column respectively.

Meanwhile, in some cases, it is helpful to analysis and implement some algorithm induced by norm minimization via introducing the definition of dual norm of $\|\mathbf{X}\|_{\mathcal{A}_m}$, which is defined as

$$\begin{aligned} \|\mathbf{Z}\|_{\mathcal{A}'_m} &= \sup_{\|\mathbf{X}\|_{\mathcal{A}_m} \leq 1} \langle \mathbf{Z}, \mathbf{X} \rangle_{\mathbb{R}} \\ &= \sup_{\substack{\mathbf{f}_k \in [0,1] \times [0,1] \\ \sum_k |s_k| \leq 1}} \langle \mathbf{Z}, \sum_k s_k \mathbf{A}_d(\mathbf{f}_k) \rangle_{\mathbb{R}} \\ &= \sup_{\mathbf{f} \in [0,1] \times [0,1]} \langle \mathbf{Z}, \mathbf{A}_m(\mathbf{f}) \rangle_{\mathbb{R}} \end{aligned} \quad (21)$$

Here, $(\mathcal{A}'_m, \|\cdot\|_{\mathcal{A}'_m})$ and $(\mathcal{A}_m, \|\cdot\|_{\mathcal{A}_m})$ are dual normal space to each other. By weak duality, it always holds that

$$|\langle \mathbf{X}, \mathbf{Z} \rangle| \leq \|\mathbf{Z}\|_{\mathcal{A}'_m} \cdot \|\mathbf{X}\|_{\mathcal{A}_m} \quad (22)$$

III. MANM ALGORITHM FOR 2D DOA

In this section, we consider two issues about 2D spectrum estimation and denoising via matrix atomic norm minimization from partial or noisy observations, i.e, (a) recovering the original completed data \mathbf{X}^\sharp from their partial noiseless observations \mathbf{X}_Ω ; and (b) denoising from their full observations \mathbf{X} in AWGN model.

A. Signal Recovery From Partial Noiseless Observations

Assume that a random or deterministic (sub)set of entries of data \mathbf{X}_Ω defined in (5) and (6) are observed, and the index set of observation entries is denoted by $\Omega \subset \{1, 2, \dots, M\} \times \{1, 2, \dots, N\}$. In the noise free case, the real complete data matrix \mathbf{X}^\sharp can be recovered from its partially observed entries via MANM problem as following

$$\mathbf{X} = \underset{\mathbf{X}}{\text{argmin}} \|\mathbf{X}\|_{\mathcal{A}_m} \quad \text{s.t.} \quad \mathbf{X}_\Omega = \mathbf{X}_\Omega^\sharp. \quad (23)$$

where, \mathbf{X}_Ω denotes the entries of \mathbf{X} whose index are in set Ω . According to theorem 1 optimum problem (23) can be solved via following semidefinite program,

$$\begin{aligned} \underset{(\mathbf{u}, \mathbf{v}, \mathbf{X})}{\text{argmin}} \quad & \text{Tr} \left(\frac{1}{2M} \mathcal{T}(\mathbf{u}) + \frac{1}{2N} \mathcal{T}(\mathbf{v}) \right) \\ \text{s.t.} \quad & \begin{bmatrix} \mathcal{T}(\mathbf{u}) & \mathbf{X} \\ \mathbf{X}^H & \mathcal{T}(\mathbf{v}) \end{bmatrix} \succeq \mathbf{0} \\ & \mathbf{X}_\Omega = \mathbf{X}_\Omega^\sharp. \end{aligned} \quad (24)$$

It is easy to solve this SDP problem by using CVX soft parcel [28]. While, in order to seek the uniqueness condition for solution of problem (23), we resort to analysis its dual problem. According to (21) it can be obtained that the dual problem of (23) is

$$\max_{\mathbf{Z}} |\langle \mathbf{Z}, \mathbf{X}^\sharp \rangle| \quad \text{s.t.} \quad \|\mathbf{Z}\|_{\mathcal{A}'_m} \leq 1, \quad \mathbf{Z}_{\Omega^c} = \mathbf{0} \quad (25)$$

where $\Omega^c \triangleq \{1, 2, \dots, M\} \times \{1, 2, \dots, N\} \setminus \Omega$ denotes the complementary index set of Ω .

Let (\mathbf{X}, \mathbf{Z}) be primal-dual feasible solution to (23) and (25), then $|\langle \mathbf{Z}, \mathbf{X} \rangle| = |\langle \mathbf{Z}, \mathbf{X}^\sharp \rangle| = \|\mathbf{X}^\sharp\|_{\mathcal{A}_m}$ holds if and only if \mathbf{Z} is

dual optimal and \mathbf{X} is primal optimal. Utilizing strong duality, we have the following proposition to certify the optimality of the solution of (23).

Proposition 1 *The solution of optimum problem (23) is unique and equal to the complete data $\mathbf{X}^\sharp = \sum_{j \in J} s_j \mathbf{A}_m(\mathbf{f}_j)$ if there exists \mathbf{Z} and $Q(\mathbf{f}) \triangleq \langle \mathbf{Z}, \mathbf{A}_m(\mathbf{f}) \rangle$ that satisfying*

$$\begin{cases} \mathbf{Z}_{\Omega^c} = \mathbf{0} \\ Q(\mathbf{f}_j) = \text{sign}(s_j), \quad \forall \mathbf{f}_j \in \mathcal{F} \\ |Q(\mathbf{f})| < 1, \quad \forall \mathbf{f} \notin \mathcal{F} \end{cases} \quad (26)$$

where, $\mathcal{F} = \{\mathbf{f}_j\}_{j \in J}$ which including all 2D-frequency components of \mathbf{X}^\sharp .

Proof: First, any \mathbf{Z} satisfying (26) is dual feasible. one has $\|\mathbf{Z}\|_{\mathcal{A}'_m} \leq 1$ and

$$\begin{aligned} \|\mathbf{X}^\sharp\|_{\mathcal{A}_m} &\geq \|\mathbf{X}^\sharp\|_{\mathcal{A}_m} \|\mathbf{Z}\|_{\mathcal{A}'_m} \geq |\langle \mathbf{Z}, \mathbf{X}^\sharp \rangle| \\ &= |\langle \mathbf{Z}, \sum_{j \in J} s_j \mathbf{A}_m(\mathbf{f}_j) \rangle| = |\sum_{j \in J} s_j^* \langle \mathbf{Z}, \mathbf{A}_m(\mathbf{f}_j) \rangle| \\ &= |\sum_{j \in J} s_j^* Q(\mathbf{f}_j)| = \sum_{j \in J} |s_j| \geq \|\mathbf{X}^\sharp\|_{\mathcal{A}_m}. \end{aligned} \quad (27)$$

Hence $|\langle \mathbf{Z}, \mathbf{X}^\sharp \rangle| = \|\mathbf{X}^\sharp\|_{\mathcal{A}_m}$. By strong duality it holds that \mathbf{X}^\sharp is primal optimal and \mathbf{Z} is dual optimal.

For uniqueness, assume that $\hat{\mathbf{X}} = \sum_j \hat{s}_j \mathbf{A}_m(\hat{\mathbf{f}}_j)$ with $\|\hat{\mathbf{X}}\|_{\mathcal{A}_m} = \sum_j |\hat{s}_j|$ is another optimal solution. Then one has

$$\begin{aligned} |\langle \mathbf{Z}, \hat{\mathbf{X}} \rangle| &= |\langle \mathbf{Z}, \sum_j \hat{s}_j \mathbf{A}_m(\hat{\mathbf{f}}_j) \rangle| \\ &= |\sum_{\hat{\mathbf{f}}_j \in \mathcal{F}} \hat{s}_j^* \langle \mathbf{Z}, \mathbf{A}_m(\hat{\mathbf{f}}_j) \rangle + \sum_{\hat{\mathbf{f}}_l \notin \mathcal{F}} \hat{s}_l^* \langle \mathbf{Z}, \mathbf{A}_m(\hat{\mathbf{f}}_l) \rangle| \\ &\leq \sum_{\hat{\mathbf{f}}_j \in \mathcal{F}} |\hat{s}_j| + \sum_{\hat{\mathbf{f}}_l \notin \mathcal{F}} |\hat{s}_l| = \|\hat{\mathbf{X}}\|_{\mathcal{A}_m} \end{aligned}$$

which contradicts strong duality. Therefore the optimal solution of (23) is unique. \blacksquare

Proposition 1 is a sufficient condition other than necessary condition to guarantee the uniqueness of optimality solution for problem (23), i.e., as long as we can find a dual polynomial that satisfies (26), then $\mathbf{X} = \mathbf{X}^\sharp$ is the unique optimum solution of problem (23). while, the inverse claims not necessarily hold.

Remark 1: Reducing Complexity: The MANM-SDP (55) is to solving SDP problem from a constraint of size $(M + N) \times (M + N)$, while as for the vectorial ANM-SDP (15) the constraint size is $(MN + 1) \times (MN + 1)$. Hence the MANM method is able to remarkably decrease the constraint size in SDP especially when the dimension of array (M, N) are very large. This also can be seen in their time consuming level in simulation results in section IV.

Remark 2: 2D-Frequencies estimation: It is often the case that the harmonic components \mathbf{f} are more focused than the completeness of the observation data matrix \mathbf{X} . while the MANM-SDP algorithm (55) offers us a way to directly recover the harmonic components information of

$\mathbf{f}^\sharp = \{(f_{x,i}^\sharp, f_{y,i}^\sharp)\}_{i=1,\dots,K}$ from $\mathcal{T}(\mathbf{u})$ and $\mathcal{T}(\mathbf{v})$ via

$$\begin{cases} \mathcal{T}(\mathbf{u}) = \mathbf{A}_{x(\mathbf{f}_x^\sharp)} \cdot \mathbf{D}_x \cdot \mathbf{A}_{x(\mathbf{f}_x^\sharp)}^T, & \mathbf{D}_x \succ \mathbf{0} \\ \mathcal{T}(\mathbf{v}) = \mathbf{A}_{y(\mathbf{f}_y^\sharp)} \cdot \mathbf{D}_y \cdot \mathbf{A}_{y(\mathbf{f}_y^\sharp)}^T, & \mathbf{D}_y \succ \mathbf{0}. \end{cases} \quad (28)$$

Remark 3: 2D-Frequencies Pairing: By solving the SDP in (55), the 2D harmonic information can be obtained via Vandermonde decomposition on their one-level Toeplitz matrices, which is much simpler than the two-level decomposition in [10], [11], and then pairing the harmonic components into K pairs by maximum correlation method as following,

$$j_i = \underset{j}{\text{argmax}} \quad |\mathbf{a}_{x(f_{x,i}^\sharp)}^H \cdot \hat{\mathbf{X}} \cdot \mathbf{a}_{y(f_{y,j}^\sharp)}^*|. \quad (29)$$

where, j_i denotes the frequency index of \mathbf{f}_y that matched to $f_{x,i}$, and $\hat{\mathbf{X}}$ denotes the recovered data matrix.

B. Signal Denoise From Full Observed Data

In this section, we consider the problem of 2D DOA in additive noise case when full observations are available with theirs observation model given as

$$\mathbf{Y} = \mathbf{X}^\sharp + \mathbf{W} \quad (30)$$

where, $\mathbf{W} = [w_{i,j}]_{M \times N} \in \mathbb{C}^{M \times N}$ is the noise data part, \mathbf{X}^\sharp is the real complete data part. In this case, the matrix atomic norm regularized recovery method is proposed as

$$\hat{\mathbf{X}} = \underset{\mathbf{X}}{\text{argmin}} \frac{1}{2} \|\mathbf{Y} - \mathbf{X}\|_F^2 + \lambda \|\mathbf{X}\|_{\mathcal{A}_m} \quad (31)$$

here, λ is a positive regularization parameter. It is easy to see that (31) is equivalent to seek the following SDP problem

$$\begin{aligned} &\underset{(\mathbf{u}, \mathbf{v}, \mathbf{X})}{\text{argmin}} \quad \frac{1}{2} \|\mathbf{Y} - \mathbf{X}\|_F^2 + \lambda \text{Tr} \left(\frac{1}{2M} \mathcal{T}(\mathbf{u}) + \frac{1}{2N} \mathcal{T}(\mathbf{v}) \right) \\ &s.t. \quad \begin{bmatrix} \mathcal{T}(\mathbf{u}) & \mathbf{X} \\ \mathbf{X}^H & \mathcal{T}(\mathbf{v}) \end{bmatrix} \succeq \mathbf{0}. \end{aligned} \quad (32)$$

The above algorithm can be efficiently implemented via utilizing CVX tool [28]. Meanwhile, the 2D-frequency components can be obtained via the same Vandermonde decomposing methods for Toeplitz matrices $\mathcal{T}(\mathbf{u}), \mathcal{T}(\mathbf{v})$ that are dealt with in (28) and paired technique in (29).

In order to guarantee the correctness of the denoising and estimation algorithm (32), two useful propositions about Optimal solution condition and error bound for (31) are concluded as the following, with their proofs are given in Appendix B.

Proposition 2 (Optimality Conditions) *If $\hat{\mathbf{X}}$ is the solution of (31) then it holds that*

$$\begin{cases} \|\mathbf{Y} - \hat{\mathbf{X}}\|_{\mathcal{A}'_m} \leq \lambda \\ \langle \mathbf{Y} - \hat{\mathbf{X}}, \hat{\mathbf{X}} \rangle = \lambda \|\hat{\mathbf{X}}\|_{\mathcal{A}_m}. \end{cases} \quad (33)$$

Proposition 3 (Error Bound) *If $\|\mathbf{W}\|_{\mathcal{A}'_m} \leq \lambda$, then the optimum solution $\hat{\mathbf{X}}$ of (31) satisfies*

$$\|\hat{\mathbf{X}} - \mathbf{X}^\sharp\|_F^2 \leq 2\lambda \|\mathbf{X}^\sharp\|_{\mathcal{A}_m}. \quad (34)$$

It is often the case that the observed noises are random noise, hence it can be obtained that expected error rate of

estimation in (31) is as following whose proof is detailed in Appendix B.

Theorem 2 Assume the entries of \mathbf{W} are i.i.d. Gaussian entries with $w_{i,j} \sim \mathcal{CN}(0, \sigma^2)$, let

$$\lambda = 2\sigma\sqrt{MN} \left(\sqrt{\ln[16\pi^2(M-1)(N-1)]} + \frac{128\pi^2(M-1)^2(N-1)^2}{\sqrt{\ln[16\pi^2(M-1)(N-1)]}} \right) \quad (35)$$

then the expected mean square error of solution $\hat{\mathbf{X}}$ to (31) is bounded as

$$\mathbb{E}\{\|\hat{\mathbf{X}} - \mathbf{X}^\sharp\|_F^2\} \leq 2\lambda\|\mathbf{X}^\sharp\|_{\mathcal{A}_m}. \quad (36)$$

Note that, in the above theorem λ is proportional to the noise standard deviation σ , which implies the weaker the noise level the more precious the estimation accuracy of data recovery is.

IV. NUMERICAL EXPERIMENTS

In this section, three kinds of experiments are conducted to verify the efficiency and examine the performance of the proposed algorithms (24) and (32).

A. MANM Recovery from Partial noiseless observation (24)

In this experiment, the dimension of array is set as $M = N = 10$, for these 2D-harmonic signals that included in the received data matrix \mathbf{X} , their 2D-frequency pair of $f_{x,i}$ and $f_{y,i}$ are randomly located in $[0, 1] \times [0, 1]$ satisfy the separation condition $\Delta = \min \max_{i \neq k} \{|f_{x,i} - f_{x,k}|, |f_{y,i} - f_{y,k}|\} > \frac{1.19}{M}$ as in [25], and their signal amplitude $\mathbf{s} \in \mathbb{C}^K$ satisfy i.i.d. complex Gaussian distribution. Each entry in \mathbf{X}^\sharp was observed with equal probability of $p = \frac{|\Omega|}{MN}$ via sub-Nyquist sampling, where Ω is the index set of observation entries and $|\Omega|$ denotes the number of observation entries in \mathbf{X}^\sharp . All simulation for algorithm (24) was implemented using CVX [28]. The performance of recovery algorithm (24) are evaluated by the normalized reconstruction error as $\frac{\|\hat{\mathbf{X}} - \mathbf{X}^\sharp\|_F}{\|\mathbf{X}^\sharp\|_F}$, and the reconstruction is considered to be successful if its reconstruction error less than 10^{-4} .

The successful recovery rates are obtained from average results of conducting a total of 300 trials, then successful recovery rate versus the number of observation entries $|\Omega|$ are shown in Fig. 2 and Fig. 3 with $K = 2, 4, 6, 8$ respectively. It can be seen that the more the observation entries are, the higher the success rate becomes for the same sparsity level. And the larger the number of 2D-frequency pairs is the lower the successful recovery rate turns for the same observation level p .

B. MANM denoise from full noise data (32)

In this experiment, the dimension of array is set as $M = N = 12$ and the number of 2D-harmonic signals is set to $K = 6$ and their 2D-frequencies are randomly generated frequency pairs in $[0, 1] \times [0, 1]$ to satisfy the separation condition $\Delta > \frac{1.19}{M}$. Meanwhile the coefficient of each frequency was generated with constant magnitude one and a random phase from $[0, 2\pi]$. The noise matrix \mathbf{W} is randomly generated with

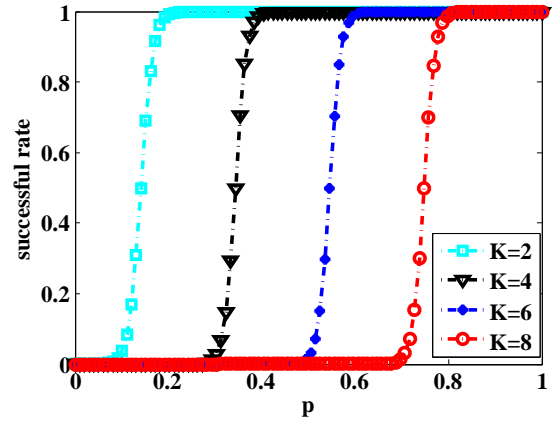


Fig. 2. Successful rate of reconstruction versus efficient observation rate p for $K = 2, 4, 6, 8$ when $M = N = 10$.

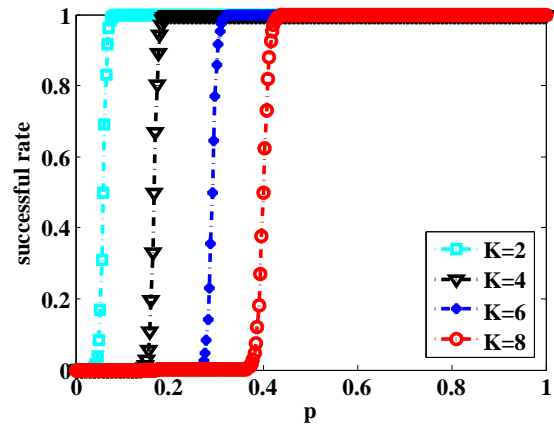


Fig. 3. Successful rate of reconstruction versus efficient observation rate p for $K = 2, 4, 6, 8$ when $M = N = 18$.

i.i.d. complex Gaussian distribution, i.e., $w_{i,j} \sim \mathcal{CN}(0, \sigma^2)$. The vector mean square error (MSE) of the data matrix denoising estimation is defined as $\text{MSE}(\hat{\mathbf{X}}) \triangleq \mathbb{E}\|\hat{\mathbf{X}} - \mathbf{X}^\sharp\|_F^2$ and obtained via taking average of 300 independent trials. The Signal-Noise-Ratio (SNR) is defined as $\text{SNR} \triangleq \frac{1}{\sigma^2}$.

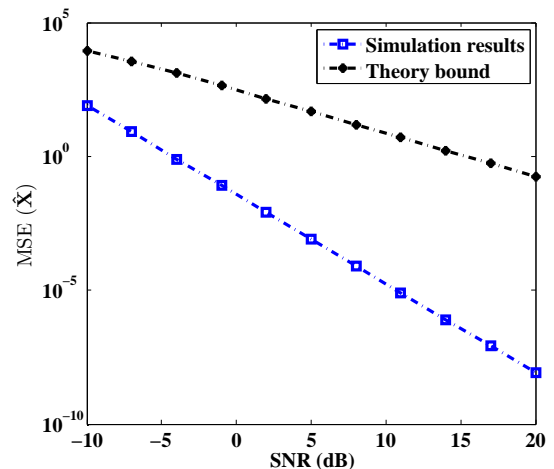


Fig. 4. The MSE performance for data matrix \mathbf{X} denoising via MANM method, and its theoretical upper bound, versus different SNR level when $M = N = 12, K = 6$.

Fig. 4 shows the MSE performance of algorithm (31) as well as the theoretical upper bound (36) obtained from Theorem 2, which can be seen that the MSE of data matrix denoising estimation decreases with the increasing of SNR. Meanwhile, the theoretical bound exhibits similar trends as the simulation performance, though it's not sharp, it is an upper bound for data matrix estimation.

Furthermore, the performance of 2D frequency component estimation of (2) are evaluated with comparison against the Cramer-Rao-Bound (CRB). And the MSE of estimation is measured as

$$\text{MSE}(\hat{\mathbf{f}}) = \mathbb{E}\|\hat{\mathbf{f}} - \mathbf{f}^\# \|^2 = \mathbb{E} \sum_{i=1}^K [(\hat{f}_{x,i} - f_{x,i}^\#)^2 + (\hat{f}_{y,i} - f_{y,i}^\#)^2]$$

where, $\hat{\mathbf{f}}$ and $\mathbf{f}^\#$ are the estimated 2D-frequency vector and the true 2D frequency vector respectively. And the simulated MSE of 2D-frequency estimation is obtained via averaging over 500 Monte Carlo runs with respect to the noise realization, while the CRB of 2D-frequency $\mathbf{f}^\#$ can be derived from the Fisher information matrix as is in [8].

Fig. 5 shows the average MSE of 2D-frequency and the corresponding CRB with respect to different SNR level. It can be seen that, with the increase of SNR level, the average MSE of 2D-frequency estimation gradually approaches to 0.

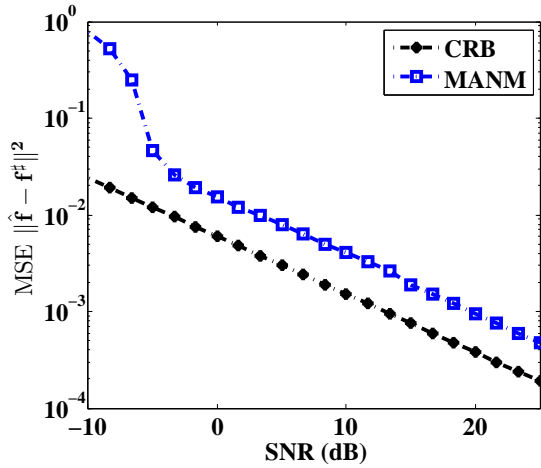


Fig. 5. The MSE performance for 2D-frequency estimation via MANM method, and its CRB, versus different SNR level when $M = N = 12$, $K = 6$.

C. Comparisons With Existing Approaches

In this experiment, the performance of proposed MANM method for 2D-frequency estimation are compared with vectorial ANM [25] and other gridless sparse method such as basis pursuit (BP) and orthogonal matched pursuit (OMP) method. As for vectorial ANM method the VANM 2D-DOA is to solve

$$\hat{\mathbf{X}} = \underset{\mathbf{X}}{\text{argmin}} \frac{1}{2} \|\mathbf{Y} - \mathbf{X}\|_F^2 + \lambda \|\mathbf{X}\|_{\mathcal{A}_v} \quad (37)$$

where, $\|\mathbf{X}\|_{\mathcal{A}_v}$ is defined as in (15) and the 2D-frequency are obtained via matrix enhancement matrix pencil (MEMP) method [8].

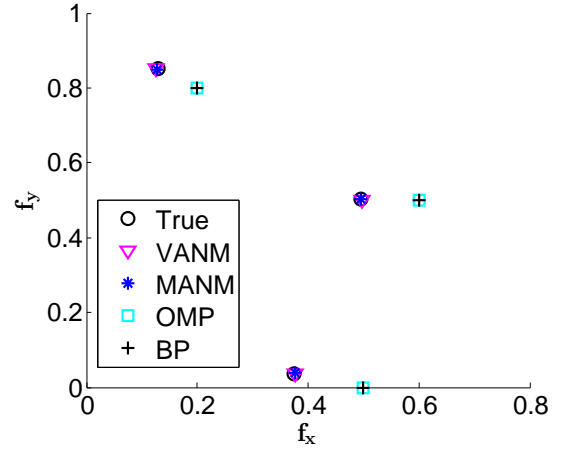


Fig. 6. The 2D-frequencies estimation via different methods ($M = N = 10$, $K = 3$, SNR = 6dB, $M_x = N_y = 10$)

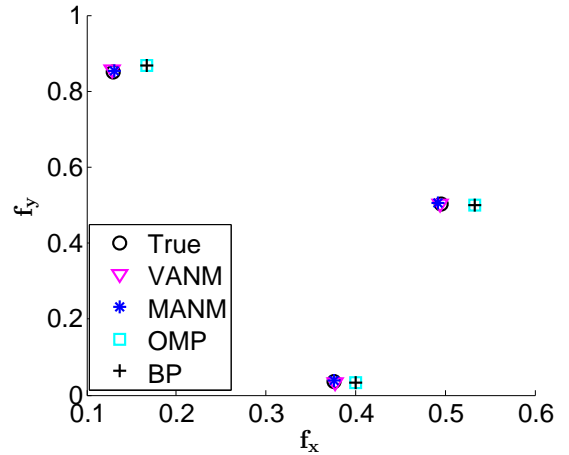


Fig. 7. The 2D-frequencies estimation via different methods ($M = N = 10$, $K = 3$, SNR = 6dB, $M_x = N_y = 30$)

By split the 2D-frequency plane $[0, 1] \times [0, 1]$ into a large number of discrete grids, then grid BP method can be applied to (30) as

$$\underset{\mathbf{s} \in \mathbb{C}^T}{\text{argmin}} \|\mathbf{s}\|_1 \quad s.t. \quad \mathbf{y} = \Phi \mathbf{s} + \mathbf{w} \quad (38)$$

where, $\Phi = \mathbf{A}_y(\mathbf{f}_y) \otimes \mathbf{A}_x(\mathbf{f}_x)$, $\mathbf{s} = \text{vec}(\mathbf{S})$ and $\mathbf{w} = \text{vec}(\mathbf{W})$ are based on (6). The interval $[0, 1] \times [0, 1]$ is divided into $M_x \times N_y$ grids to implement BP method as well as OMP method.

In order to compare the MSE performance of 2D - frequencies estimation via different methods, the parameters are set as SNR = 6dB, and the 2D-frequencies are randomly generated in $[0, 1) \times [0, 1)$, with $\{f_{x,k}, f_{y,k}\}_{k=1:3} = \{(0.49546, 0.50402), (0.37560, 0.00369), (0.12951, 0.85163)\}$ where the coefficient of each frequency was generated with constant magnitude one and a random phase from $[0, 2\pi)$. Typical 2D-frequencies estimation result for different methods are shown in Fig. 6 and Fig. 7, with $M_x = N_y = 10$ and $M_x = N_y = 30$, respectively. It can be seen that with the more refined the grids are the better the 2D-DOA estimation results are for OMP and BP method, and the gridless methods

of VANM and MANM methods gain better estimation accuracy than those grids methods such OMP and BP even if the grids are refined.

Furthermore, the MSE performance for 2D-frequency estimation via different methods and its CRB versus SNR are shown in Fig. 6, with all parameters are set as is in Fig. 8. The simulated MSE of are obtained via averaging over 500 Monte Carlo runs with respect to the noise realization, and are plotted together in Fig. 6. It can be seen that the MSE of all method decrease as the SNR increase. Compared with other method the MANM estimation method outperform all other method, which implies that the 2D-Frequencies estimation precision is better than others.

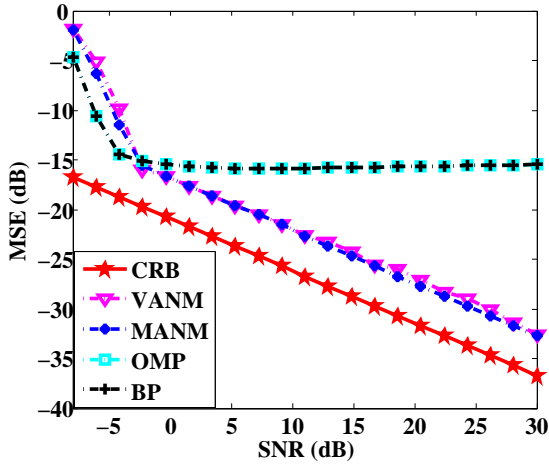


Fig. 8. The MSE performance for 2D-frequency estimation via different methods ($M = N = 10, K = 5, M_x = N_y = 100$)

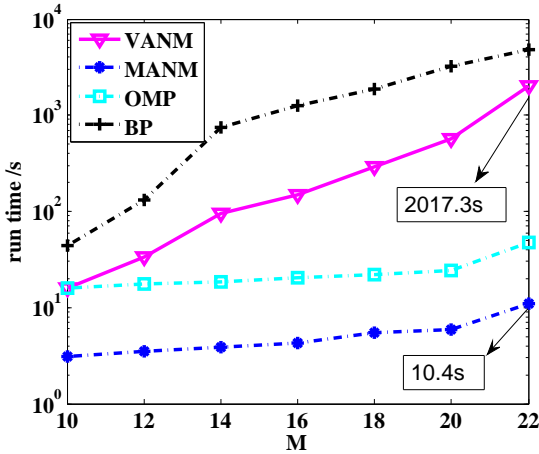


Fig. 9. The run time for 2D-frequency estimation via different methods versus array dimension M when ($K = 5, \text{SNR} = 6\text{dB}, M_x = N_y = 100$)

In the last experiment, the complexity of different algorithms are tested via their running time versus dimension of array M, N and are shown in Fig. 7. With the parameters are set as $M_x = N_y = 100, K = 5$ and $\text{SNR} = 6\text{dB}$, the experiment is conducted on a computer with Inter Core i7-3370 @3.4 GHz. It can be seen from Fig. 7 that, the time consuming of all methods increase with the increasing of the dimension of array M and N , the running time of VANM

method increases much faster than the proposed MANM method. When $M = N = 22$, the running time of the VANM is 2017.3s, while that of the MANM is only 10.4s. what's more, when the dimension of array is reach $M = N = 35$ it takes almost a week to complete even one trial via VANM method, therefore, the MANM method earns a huge benefit in computational efficiency for large-scale arrays as well as retain high accuracy in 2D-Frequencies estimation.

V. CONCLUSIONS

In this paper, the problem of 2D-spectrum estimation and denoising 2D spectrally-sparse signals from their partial observations are studied, two approaches are developed and solved efficiently from matrix atomic norm minimizing via semi-definite programming other than vectorial atomic norm minimizing. The first algorithm aims to recover the full signal matrix from its partial observation, and the second algorithm aims to recover the structured signal matrix from full noise signal matrix. Theoretical performance guarantees are derived for both approaches under different conditions. Plenty of experiments are conducted to demonstrate the efficiency of the proposed method, which greatly reduces the time spent on problem solving in large-scale array compared with the vectorial atomic norm minimizing, and retain the benefit of high estimation precision of atomic norm minimizing in 2D-Frequencies estimation.

VI. APPENDIX A USEFUL LEMMAS

In this section we introduce a few useful lemmas, that will be used in our proofs.

Lemma 1 (Carthodory-toeplitz [21], [22]) Any positive semidefinite Toeplitz matrix $\mathbf{T} \in \mathbb{C}^{N \times N}$ with $\text{rank}(\mathbf{T}) = r < N$, can be uniquely decomposed as

$$\mathbf{T} = \mathbf{V}\mathbf{D}\mathbf{V}^H$$

$$\mathbf{V} = \begin{bmatrix} 1 & 1 & \dots & 1 \\ v_1 & v_2 & \dots & v_r \\ \vdots & \vdots & \dots & \vdots \\ v_1^N & v_2^N & \dots & v_r^N \end{bmatrix}$$

$$\mathbf{D} = \text{diag}(d_1, d_2, \dots, d_r)$$

$$\text{where } \begin{cases} d_i > 0, |v_i| = 1 \\ v_i \neq v_j, \forall i \neq j \end{cases} \quad i = 1, 2, \dots, r.$$

Lemma 2 (Bernstein complex inequality [29]) Let $P(z) = \sum_{k=0}^n p_k z^k$ be a polynomial with $\text{deg}(P(z)) = n$, $p_k \in \mathbb{C}$, then

$$\sup_{|z| \leq 1} |P'(z)| \leq n \sup_{|z| \leq 1} |P(z)| \quad (39)$$

Lemma 3 (Subdifferential of norm fuction [31] [32]) $\forall \mathbf{x} \in \mathbb{X} \subseteq \mathbb{C}^N$, the subdifferential of $\|\mathbf{x}\|_{\mathbb{X}}$ is

$$\partial \|\mathbf{x}_0\|_{\mathbb{X}} = \begin{cases} \{\mathbf{g} | \mathbf{g}^H \mathbf{x}_0 = \|\mathbf{x}_0\|_{\mathbb{X}}, \|\mathbf{g}\|_{\mathbb{X}'} = 1, \mathbf{g} \in \mathbb{C}^N\} & \mathbf{x}_0 \neq \mathbf{0} \\ \{\mathbf{g} | \|\mathbf{g}\|_{\mathbb{X}'} \leq 1, \mathbf{g} \in \mathbb{C}^N\} & \mathbf{x}_0 = \mathbf{0}. \end{cases}$$

where $(\mathbb{X}', \|\cdot\|_{\mathbb{X}'})$ is the dual normal space of $(\mathbb{X}, \|\cdot\|_{\mathbb{X}})$.

Lemma 4 (Bounded polynomials [33])

Let $H(w) = \sum_{k=0}^{K-1} h_k e^{-jk w}$, $\mathbf{h} = [h_0, h_1, \dots, h_{K-1}]^T$, then

$$|H(w)| \leq \gamma, \quad \forall w \in [0, 2\pi] \quad (40)$$

holds, iff

$$\left\{ \begin{array}{l} \exists \mathbf{Q} \in \mathbb{C}^{K \times K}, \mathbf{Q} = \mathbf{Q}^H \\ \gamma^2 \delta_k = \text{Tr}(\Theta_k \mathbf{Q}), \quad k = 0 : K-1 \\ \begin{bmatrix} \mathbf{Q} & \mathbf{h} \\ \mathbf{h}^H & \mathbf{Q} \end{bmatrix} \succeq \mathbf{0} \end{array} \right. \quad (41)$$

where, $\Theta_k \in \mathbb{C}^{K \times K}$ is the elementary Toeplitz matrix with ones on the k -th diagonal and zeros elsewhere. i.e.,

$$\Theta_k = \begin{array}{c} | \text{---} \text{---} \text{---} \text{---} \text{---} \rightarrow k \\ \begin{bmatrix} 0 & \cdots & 0 & 1 & 0 & \cdots & \cdots & 0 \\ 0 & 0 & \cdots & 0 & 1 & 0 & \cdots & 0 \\ \vdots & \ddots & \ddots & \cdots & 0 & \ddots & \cdots & 0 \\ \vdots & \vdots & \ddots & \ddots & \cdots & \cdots & 1 & 0 \\ \mathbf{0} & \mathbf{0} & \mathbf{0} & \mathbf{0} & \mathbf{0} & \ddots & \mathbf{0} & \mathbf{1} \\ \vdots & \ddots & \ddots & \ddots & \ddots & \ddots & \ddots & \mathbf{0} \end{bmatrix} \end{array} \quad (42)$$

Lemma 5 (Bounded polynomials with matrix coefficients [33]) Let $\mathbf{H}_a(\theta) = \mathbf{H}\mathbf{a}(\theta)$, $\mathbf{a}(\theta) = [1, e^{-j\theta}, \dots, e^{-j(K-1)\theta}]^T$, then

$$\sigma_{\max}(\mathbf{H}_a(\theta)) \leq \gamma, \quad \forall \theta \in [0, 2\pi] \quad (43)$$

holds, iff

$$\left\{ \begin{array}{l} \exists \mathbf{Q} \in \mathbb{C}^{K \times K}, \mathbf{Q} = \mathbf{Q}^H \\ \gamma^2 \delta_k = \text{Tr}(\Theta_k \mathbf{Q}), \quad k = 0 : K-1 \\ \begin{bmatrix} \mathbf{Q} & \mathbf{H} \\ \mathbf{H}^H & \mathbf{I}_K \end{bmatrix} \succeq \mathbf{0} \end{array} \right. \quad (44)$$

where, $\Theta_k \in \mathbb{C}^{K \times K}$ is the elementary Toeplitz matrix with ones on the k -th diagonal and zeros elsewhere, which is same as in (42).

VII. APPENDIX B PROOF OF THEOREM 1

A. equivalent condition of dual norm

Proposition 4 Let $\mathbf{Z} \in \mathbb{C}^{M \times N}$ and $\|\mathbf{Z}\|_{\mathcal{A}'_m}$ be the dual norm of matrix atomic norm that defined as in (21) then

$$\|\mathbf{Z}\|_{\mathcal{A}'_m} \leq 1 \quad \Leftrightarrow \left\{ \begin{array}{l} \exists \mathbf{P} \in \mathbb{C}^{N \times N}, \mathbf{Q} \in \mathbb{C}^{M \times M}, \mathbf{P} = \mathbf{P}^H, \mathbf{Q} = \mathbf{Q}^H \\ \delta_n = \text{Tr}(\Theta_n^{(1)} \mathbf{P}), \quad n = 0 : N-1 \\ \delta_m = \text{Tr}(\Theta_m^{(2)} \mathbf{Q}), \quad m = 0 : M-1 \\ \begin{bmatrix} \mathbf{Q} & \mathbf{Z} \\ \mathbf{Z}^H & \mathbf{P} \end{bmatrix} \succeq \mathbf{0} \end{array} \right. \quad (45)$$

where, $\Theta_n^{(1)} \in \mathbb{C}^{N \times N}$ and $\Theta_m^{(2)} \in \mathbb{C}^{M \times M}$ are the elementary Toeplitz matrix with ones on the n -th diagonal and ones on the m -th diagonal, respectively, which are similar to (42).

Proof: Let

$$\left\{ \begin{array}{l} \mathbf{h}(f_x) = \mathbf{Z}\mathbf{a}_x(f_x), \mathbf{h} = \mathbf{h}(f_x) \\ H(f_y) = \mathbf{h}^H \cdot \mathbf{a}_y(f_y) = \sum_{k=0}^{N-1} h_k z^{-k} |_{z=e^{j \cdot f_y}} \end{array} \right. \quad (46)$$

then according to lemma 4, it can be obtained that

$$\|\mathbf{Z}\|_{\mathcal{A}'_m} \leq 1 \Leftrightarrow |H(f_y)| \leq 1, \forall f_y, f_x \in [0, 2\pi] \quad (47)$$

$$\Leftrightarrow \left\{ \begin{array}{l} \exists \mathbf{P} \in \mathbb{C}^{M \times M}, \mathbf{P} = \mathbf{P}^H \\ \delta_n = \text{Tr}(\Theta_n^{(1)} \mathbf{P}), \quad n = 0 : N-1 \\ \begin{bmatrix} \mathbf{P} & \mathbf{h} \\ \mathbf{h}^H & \mathbf{1} \end{bmatrix} \succeq \mathbf{0} \quad \forall f_x \in [0, 2\pi] \end{array} \right. \quad (48)$$

where, $\Theta_n^{(1)} \in \mathbb{C}^{N \times N}$ is the elementary Toeplitz matrix with ones on the n -th diagonal and zeros elsewhere. Since

$$\begin{aligned} \begin{bmatrix} \mathbf{P} & \mathbf{h} \\ \mathbf{h}^H & \mathbf{1} \end{bmatrix} \succeq \mathbf{0} &\Leftrightarrow \mathbf{1} - \mathbf{h}^H \mathbf{P}^{-1} \mathbf{h} \geq 0 \\ &\Leftrightarrow \mathbf{a}_x^H(f_x) \mathbf{Z}^H \mathbf{P}^{-1} \mathbf{Z} \cdot \mathbf{a}_x(f_x) \leq 1 \end{aligned} \quad (49)$$

Let $\mathbf{b}(f_x) \triangleq \mathbf{P}^{-\frac{1}{2}} \mathbf{Z} \cdot \mathbf{a}_x(f_x)$, then (49) is equivalent to

$$\mathbf{b}\mathbf{b}^H \preceq \mathbf{I}_M \Leftrightarrow \sigma_{\max}(\mathbf{b}(f)) \leq 1, \forall f \in [0, 2\pi] \quad (50)$$

Let $\mathbf{H}_b \triangleq \mathbf{P}^{-\frac{1}{2}} \mathbf{Z}$, then according to lemma 5, (50) is identical to

$$\left\{ \begin{array}{l} \exists \mathbf{Q} \in \mathbb{C}^{M \times M}, \mathbf{Q} = \mathbf{Q}^H \\ \delta_m = \text{Tr}(\Theta_m^{(2)} \mathbf{Q}), \quad m = 0 : M-1 \\ \begin{bmatrix} \mathbf{Q} & \mathbf{H}_b \\ \mathbf{H}_b^H & \mathbf{I}_N \end{bmatrix} \succeq \mathbf{0} \end{array} \right. \quad (51)$$

where, $\Theta_m^{(2)} \in \mathbb{C}^{M \times M}$ is the elementary Toeplitz matrix with ones on the m -th diagonal and zeros elsewhere. then it comes

$$\begin{aligned} \mathbf{Q} - \mathbf{H}_b \mathbf{H}_b^H \succeq \mathbf{0} &\Leftrightarrow \mathbf{Q} - \mathbf{Z}^H \mathbf{P}^{-1} \mathbf{Z} \succeq \mathbf{0} \\ &\Leftrightarrow \begin{bmatrix} \mathbf{Q} & \mathbf{Z} \\ \mathbf{Z}^H & \mathbf{P} \end{bmatrix} \succeq \mathbf{0} \end{aligned} \quad (52)$$

based on (48)(51)(52), it can be derived that

$$\|\mathbf{Z}\|_{\mathcal{A}'_m} \leq 1 \quad \Leftrightarrow \left\{ \begin{array}{l} \exists \mathbf{P} \in \mathbb{C}^{N \times N}, \mathbf{Q} \in \mathbb{C}^{M \times M}, \mathbf{P} = \mathbf{P}^H, \mathbf{Q} = \mathbf{Q}^H \\ \delta_n = \text{Tr}(\Theta_n^{(1)} \mathbf{P}), \quad n = 0 : N-1 \\ \delta_m = \text{Tr}(\Theta_m^{(2)} \mathbf{Q}), \quad m = 0 : M-1 \\ \begin{bmatrix} \mathbf{Q} & \mathbf{Z} \\ \mathbf{Z}^H & \mathbf{P} \end{bmatrix} \succeq \mathbf{0} \end{array} \right. \quad (53)$$

■

B. proof of theorem 1

Proof: According to the definition it holds that

$$\|\mathbf{X}\|_{\mathcal{A}_m} = \sup_{\|\mathbf{Z}\|_{\mathcal{A}'_m} \leq 1} |\text{Tr}(\mathbf{X}^H \mathbf{Z})| = \sup_{\|\mathbf{Z}\|_{\mathcal{A}'_m} \leq 1} \text{Re}[\text{Tr}(\mathbf{X}^H \mathbf{Z})] \quad (54)$$

then according to proposition 4 it can be obtained that

$$\|\mathbf{X}\|_{\mathcal{A}_m} = \sup \text{Re}[\text{Tr}(\mathbf{X}^H \mathbf{Z})] \quad \text{s.t.} \begin{cases} \exists \mathbf{P} \in \mathbb{C}^{N \times N}, \mathbf{Q} \in \mathbb{C}^{M \times M}, \mathbf{P} = \mathbf{P}^H, \mathbf{Q} = \mathbf{Q}^H \\ \delta_n = \text{Tr}(\mathbf{\Theta}_n^{(1)} \mathbf{P}), \quad n = 0 : N - 1 \\ \delta_m = \text{Tr}(\mathbf{\Theta}_m^{(2)} \mathbf{Q}), \quad m = 0 : M - 1 \\ \begin{bmatrix} \mathbf{Q} & \mathbf{Z} \\ \mathbf{Z}^H & \mathbf{P} \end{bmatrix} \succeq \mathbf{0} \end{cases} \quad (55)$$

the Lagrange augment function of (55) is

$$\begin{aligned} L(\mathbf{Q}, \mathbf{P}, \mathbf{Y}, \mathbf{Z}, \mathbf{T}_1, \mathbf{T}_2) &= -\frac{1}{2} \text{Tr}(\mathbf{X}^H \mathbf{Z} + \mathbf{Z}^H \mathbf{X}) - \sum_{n=0}^N \mu_n (\delta_n - \text{Tr}(\mathbf{\Theta}_n^{(1)} \mathbf{P})) \\ &\quad - \sum_{m=0}^M \eta_m (\delta_m - \text{Tr}(\mathbf{\Theta}_m^{(2)} \mathbf{Q})) \\ &\quad + \text{Tr} \left(\begin{bmatrix} \mathbf{T}_1 & \mathbf{Y} \\ \mathbf{Y}^H & \mathbf{T}_2 \end{bmatrix} \begin{bmatrix} \mathbf{Q} & \mathbf{Z} \\ \mathbf{Z}^H & \mathbf{P} \end{bmatrix} \right) \end{aligned} \quad (56)$$

where $\begin{bmatrix} \mathbf{T}_1 & \mathbf{Y} \\ \mathbf{Y}^H & \mathbf{T}_2 \end{bmatrix} \succeq \mathbf{0}$. Then $\|\mathbf{X}\|_{\mathcal{A}_m} = -\inf L(\cdot)$ and the optimum value satisfy

$$\begin{cases} \frac{\partial L}{\partial \mathbf{Q}} = \mathbf{0} \\ \frac{\partial L}{\partial \mathbf{P}} = \mathbf{0} \\ \frac{\partial L}{\partial \mathbf{Z}} = \mathbf{0} \end{cases} \Leftrightarrow \begin{cases} \mathbf{T}_1 = \sum_{m=0}^M \eta_m \mathbf{\Theta}_m^{(2)} \\ \mathbf{T}_2 = \sum_{n=0}^N \mu_n \mathbf{\Theta}_n^{(1)} \\ \mathbf{Y} = \frac{1}{2} \mathbf{X} \end{cases} \quad (57)$$

$$\inf(L) = \inf_{\mathbf{T}_1, \mathbf{T}_2} [-(\eta_0 + \mu_0)] \quad (58)$$

according to the definition of $\mathbf{\Theta}_m^{(2)}$ and $\mathbf{\Theta}_n^{(1)}$, it can be obtained that (57) imply \mathbf{T}_1 and \mathbf{T}_2 are both Hermite positive Toeplitz matrices with vectors $\boldsymbol{\eta} = [\eta_0, \eta_1, \dots, \eta_{M-1}]^T$ and $\boldsymbol{\mu} = [\mu_0, \mu_1, \dots, \mu_{N-1}]^T$ as their first column respectively. Then it holds

$$\begin{aligned} \inf(L) &= \inf_{\mathbf{T}_1, \mathbf{T}_2} [-(\eta_0 + \mu_0)] \\ &= \inf_{(\boldsymbol{\eta}, \boldsymbol{\mu}) \in \mathbb{C}^M \times \mathbb{C}^N} \text{Tr} \left[-\frac{1}{M} \mathcal{T}(\boldsymbol{\eta}) - \frac{1}{N} \mathcal{T}(\boldsymbol{\mu}) \right] \end{aligned} \quad (59)$$

Therefore it can be obtained that

$$\begin{aligned} \|\mathbf{X}\|_{\mathcal{A}_m} &= \inf_{(\boldsymbol{\eta}, \boldsymbol{\mu}) \in \mathbb{C}^M \times \mathbb{C}^N} \text{Tr} \left[\frac{1}{M} \mathcal{T}(\boldsymbol{\eta}) + \frac{1}{N} \mathcal{T}(\boldsymbol{\mu}) \right] \\ \text{s.t.} \quad &\begin{bmatrix} \mathcal{T}(\boldsymbol{\eta}) & \frac{1}{2} \mathbf{X} \\ \frac{1}{2} \mathbf{X}^H & \mathcal{T}(\boldsymbol{\mu}) \end{bmatrix} \succeq \mathbf{0} \end{aligned} \quad (60)$$

which is equivalent to

$$\begin{aligned} \|\mathbf{X}\|_{\mathcal{A}_m} &= \inf_{(\mathbf{u}, \mathbf{v}) \in \mathbb{C}^M \times \mathbb{C}^N} \text{Tr} \left[\frac{1}{2M} \mathcal{T}(\mathbf{u}) + \frac{1}{2N} \mathcal{T}(\mathbf{v}) \right] \\ \text{s.t.} \quad &\begin{bmatrix} \mathcal{T}(\mathbf{u}) & \mathbf{X} \\ \mathbf{X}^H & \mathcal{T}(\mathbf{v}) \end{bmatrix} \succeq \mathbf{0} \end{aligned} \quad (61)$$

■

VIII. APPENDIX C

PROOF OF PROPOSITION 2,3 AND THEOREM 2

A. proof of proposition 2

Proof: Let $h(\mathbf{X}) = \frac{1}{2} \|\mathbf{Y} - \mathbf{X}\|_F^2 + \lambda \|\mathbf{X}\|_{\mathcal{A}_m}$, then it can be obtained that

$$\begin{cases} \partial h(\mathbf{X}) = (\hat{\mathbf{X}} - \mathbf{Y})^* + \lambda \mathbf{Z} \\ \mathbf{Z} \in \partial \|\mathbf{X}\|_{\mathcal{A}_m} \end{cases} \quad (62)$$

Since $\hat{\mathbf{X}}$ is the solution of (31) then it holds that

$$\mathbf{0} \in \partial h(\hat{\mathbf{X}}) \quad (63)$$

according to lemma (3) it has

$$\begin{cases} (\mathbf{Y} - \hat{\mathbf{X}})^* = \lambda \mathbf{Z} \\ \langle \hat{\mathbf{X}}, \mathbf{Z} \rangle = \|\hat{\mathbf{X}}\|_{\mathcal{A}_m} \\ \|\mathbf{Z}\|_{\mathcal{A}'_m} \leq 1 \end{cases}$$

then it turns out

$$\begin{cases} \|\mathbf{Y} - \hat{\mathbf{X}}\|_{\mathcal{A}'_m} \leq \lambda \\ \langle \mathbf{Y} - \hat{\mathbf{X}}, \hat{\mathbf{X}} \rangle = \lambda \|\hat{\mathbf{X}}\|_{\mathcal{A}_m} \end{cases}$$

■

B. proof of proposition 3

Proof: since $\mathbf{Y} = \mathbf{X}^\sharp + \mathbf{W}$ then

$$\begin{aligned} \|\hat{\mathbf{X}} - \mathbf{X}^\sharp\|_F^2 &= \langle \hat{\mathbf{X}} - \mathbf{X}^\sharp, \mathbf{W} - (\mathbf{Y} - \hat{\mathbf{X}}) \rangle \\ &= \langle \hat{\mathbf{X}} - \mathbf{X}^\sharp, \mathbf{W} - (\mathbf{Y} - \hat{\mathbf{X}}) \rangle_{\mathbf{R}} \\ &= \langle \mathbf{X}^\sharp, \mathbf{Y} - \hat{\mathbf{X}} \rangle_{\mathbf{R}} - \langle \mathbf{X}^\sharp, \mathbf{W} \rangle_{\mathbf{R}} \\ &\quad + \langle \hat{\mathbf{X}}, \mathbf{W} \rangle_{\mathbf{R}} - \langle \hat{\mathbf{X}}, \mathbf{Y} - \hat{\mathbf{X}} \rangle_{\mathbf{R}} \end{aligned} \quad (64)$$

$$\begin{aligned} &\leq \|\mathbf{Y} - \hat{\mathbf{X}}\|_{\mathcal{A}'_m} \|\mathbf{X}^\sharp\|_{\mathcal{A}_m} + \|\mathbf{W}\|_{\mathcal{A}'_m} \|\mathbf{X}^\sharp\|_{\mathcal{A}_m} \\ &\quad + \|\mathbf{W}\|_{\mathcal{A}'_m} \|\hat{\mathbf{X}}\|_{\mathcal{A}_m} - \lambda \|\hat{\mathbf{X}}\|_{\mathcal{A}_m} \end{aligned} \quad (65)$$

$$\begin{aligned} &\leq 2\lambda \|\mathbf{X}^\sharp\|_{\mathcal{A}_m} + (\|\mathbf{W}\|_{\mathcal{A}'_m} - \lambda) \|\hat{\mathbf{X}}\|_{\mathcal{A}_m} \\ &\leq 2\lambda \|\mathbf{X}^\sharp\|_{\mathcal{A}_m} \end{aligned} \quad (66)$$

where, (64) results from (22), (65) results from (33), (66) results from $\|\mathbf{W}\|_{\mathcal{A}'_m} \leq \lambda$. ■

C. proof of theorem 2

Proof: here we utilize the bounded property of the expectation of dual norm of $\|\mathbf{W}\|_{\mathcal{A}_m}$ to prove the claim. According to the definition of dual norm, one has

$$\|\mathbf{W}\|_{\mathcal{A}'_d} = \sup_{\mathbf{f} \in [0,1]^2} |\langle \mathbf{W}, \mathbf{A}_d(\mathbf{f}) \rangle| = \sup_{(f_x, f_y) \in [0,1]^2} |W(f_x, f_y)| \quad (67)$$

where

$$W(f_x, f_y) \triangleq \sum_{m=1}^M \sum_{n=1}^N w_{m,n}^* e^{-j2\pi[(m-1)f_x + (n-1)f_y]} \quad (68)$$

let $(u, v) = (e^{-j2\pi f_x}, e^{-j2\pi f_y})$ then

$$W(u, v) = \sum_{m=1}^M \sum_{n=1}^N w_{m,n}^* u^{m-1} v^{n-1} \quad |u| \leq 1, |v| \leq 1 \quad (69)$$

Note that $\forall u_1, u_2, v_1, v_2 \in \{\xi \mid |\xi| \leq 1, \xi \in \mathbb{C}\}$, it has

$$|W(u_1, v_1) - W(u_2, v_2)| \leq \|W'_u\|_\infty |u_1 - u_2| + \|W'_v\|_\infty |v_1 - v_2| \quad (70)$$

where

$$|u_1 - u_2| \leq 2\pi |f_{1x} - f_{2x}| \quad (71)$$

$$|v_1 - v_2| \leq 2\pi |f_{1y} - f_{2y}| \quad (72)$$

$$\|W'_u\|_\infty \leq (M-1)\|W\|_\infty = (M-1)\|\mathbf{W}\|_{\mathcal{A}'_m} \quad (73)$$

$$\|W'_v\|_\infty \leq (N-1)\|W\|_\infty = (N-1)\|\mathbf{W}\|_{\mathcal{A}'_m} \quad (74)$$

where, (73) and (74) follow by Bernstein's theorem [29], i.e. lemma 2. Then according to (68) to (74), it has

$$|W(f_{1x}) - W(f_{2x})| \leq 2\pi(M-1)|f_{1x} - f_{2x}| \cdot \|\mathbf{W}\|_{\mathcal{A}'_m} + 2\pi(N-1)|f_{1y} - f_{2y}| \cdot \|\mathbf{W}\|_{\mathcal{A}'_m} \quad (75)$$

Letting $f_{2x} \in \{0, \frac{1}{M_x}, \dots, \frac{M_x-1}{M_x}\}$, $f_{2y} \in \{0, \frac{1}{N_y}, \dots, \frac{N_y-1}{N_y}\}$, it can be seen that

$$\|\mathbf{W}\|_{\mathcal{A}'_m} \leq \max_{\substack{m=0, \dots, M_x-1 \\ n=0, \dots, N_y-1}} |W(e^{-j2\pi m/M_x}, e^{-j2\pi n/N_y})| + \pi \frac{M-1}{M_x} \|\mathbf{W}\|_{\mathcal{A}'_m} + \pi \frac{N-1}{N_y} \|\mathbf{W}\|_{\mathcal{A}'_m} \quad (76)$$

Therefore it has

$$\|\mathbf{W}\|_{\mathcal{A}'_d} \leq \left(1 - \pi \left(\frac{M-1}{M_x} + \frac{N-1}{N_y}\right)\right)^{-1} \cdot \max_{\substack{m=0, \dots, M_x-1 \\ n=0, \dots, N_y-1}} |W(e^{-j2\pi m/M_x}, e^{-j2\pi n/N_y})| \quad (77)$$

let $g_{m,n} = |W(e^{-j2\pi m/M_x}, e^{-j2\pi n/N_y})|$, since $w_{i,j}$ obey i.i.d. complex Gaussian distribution with $w_{i,j} \sim \mathcal{CN}(0, \sigma^2)$, then it can be obtained that $W(f_x, f_y) \sim \mathcal{CN}(0, MN\sigma^2)$ and $g_{m,n}$ satisfying Rayleigh distribution

$$p(g) = \frac{2g}{MN\sigma^2} e^{-\frac{g^2}{MN\sigma^2}} \quad g \geq 0 \quad (78)$$

which holds for $\forall 0 \leq m \leq M_x, 0 \leq n \leq N_y$, then we aim to find the minimum value of up bound of $\mathbb{E}(\max_{\substack{1 \leq m \leq M_x-1 \\ 1 \leq n \leq N_y-1}} g_{i,j})$ by suitably choosing M_x and N_y as is dealt in [23].

Therefore it can be seen that

$$\begin{aligned} \mathbb{E}(\max_{\substack{1 \leq m \leq M_x-1 \\ 1 \leq n \leq N_y-1}} g_{i,j}) &= \int_0^{+\infty} \mathbb{P}(\max_{\substack{1 \leq m \leq M_x-1 \\ 1 \leq n \leq N_y-1}} g_{m,n} \geq t) dt \\ &\leq \varepsilon + \int_\varepsilon^{+\infty} \mathbb{P}(\max_{\substack{1 \leq m \leq M_x-1 \\ 1 \leq n \leq N_y-1}} g_{m,n} \geq t) dt \\ &\leq \varepsilon + M_x N_y \int_\varepsilon^{+\infty} \mathbb{P}(g_{0,0} \geq t) dt \\ &= \varepsilon + M_x N_y \int_\varepsilon^{+\infty} e^{-\frac{t^2}{MN\sigma^2}} dt \quad (79) \end{aligned}$$

Hence letting $\varepsilon = \sigma \sqrt{MN \ln(M_x N_y)}$, then

$$\mathbb{E}(\max_{\substack{1 \leq m \leq M_x-1 \\ 1 \leq n \leq N_y-1}} g_{i,j}) \leq \sigma \sqrt{MN} \left(\sqrt{\ln(M_x N_y)} + \frac{M_x^2 N_y^2}{2\sqrt{\ln(M_x N_y)}} \right) \quad (80)$$

where, the second part of right hand side follows from inequality

$$\int_u^{+\infty} e^{-t^2/2} dt \leq \frac{1}{u} e^{-u^2/2} \quad u > 0 \quad (81)$$

then it can be obtained that

$$\mathbb{E}\{\|\mathbf{W}\|_{\mathcal{A}'_m}\} \leq \frac{\sigma \sqrt{MN} \left(\sqrt{\ln(M_x N_y)} + \frac{M_x^2 N_y^2}{2\sqrt{\ln(M_x N_y)}} \right)}{1 - \pi \left(\frac{M-1}{M_x} + \frac{N-1}{N_y} \right)} \quad (82)$$

let $M_x = 4\pi(M-1)$, $N_y = 4\pi(N-1)$ then

$$\begin{aligned} \mathbb{E}\{\|\mathbf{W}\|_{\mathcal{A}'_d}\} &\leq 2\sigma \sqrt{MN} \left(\sqrt{\ln[16\pi^2(M-1)(N-1)]} \right. \\ &\quad \left. + \frac{128\pi^2(M-1)^2(N-1)^2}{\sqrt{\ln[16\pi^2(M-1)(N-1)]}} \right) \quad (83) \end{aligned}$$

Let

$$\begin{aligned} \lambda &= 2\sigma \sqrt{MN} \left(\sqrt{\ln[16\pi^2(M-1)(N-1)]} \right. \\ &\quad \left. + \frac{128\pi^2(M-1)^2(N-1)^2}{\sqrt{\ln[16\pi^2(M-1)(N-1)]}} \right) \end{aligned}$$

then, it can be seen that $\mathbb{E}\{\|\mathbf{W}\|_{\mathcal{A}'_m}\} \leq \lambda$, according to proposition 3, it holds that

$$\mathbb{E}\{\|\hat{\mathbf{X}} - \mathbf{X}^\# \|_F^2\} \leq 2\lambda \|\mathbf{X}^\#\|_{\mathcal{A}_d}$$

■

REFERENCES

- [1] M. I. Skolnik, "Introduction to Radar System," 3rd ed. New York: McGraw-Hill, 2002.
- [2] J. Li and P. Stoica, "MIMO radar with colocated antennas: Review of some recent work," *IEEE Signal Process. Mag.*, vol. 24, pp. 106C114, Sep. 2007.
- [3] A. M. Sayeed and B. Aazhang, "Joint multipath-doppler diversity in mobile wireless communications," *IEEE Trans. Commun.*, no. 1, pp. 123C132, Jan. 1999.
- [4] D. Tse and P. Viswanath, "Fundamentals of Wireless Communication," Cambridge, U.K.: Cambridge Univ. Press, 2005.
- [5] R. Willett, M. Duarte, M. Davenport, and R. Baraniuk, "Sparsity and structure in hyperspectral imaging: Sensing, reconstruction, and target detection," *IEEE Signal Processing Mag.*, vol. 31, no. 1, pp. 116C126, Jan. 2014.

- [6] M. Haardt, M. Zoltowski, C. Mathews, J. Nosssek, "2D unitary ESPRIT for efficient 2D parameter estimation," *Proc. IEEE Int. Conf. Acoust. Speech Signal Process.* vol. 3, pp. 2096-2099, 1995.
- [7] Y. Hua, "A pencil-music algorithm for finding two-dimensional angles and polarizations using crossed dipoles," *IEEE Trans. Antennas Propag.*, vol. 41, no. 3, pp. 370-376, 1993.
- [8] Y. Hua, "Estimating two-dimensional frequencies by matrix enhancement and matrix pencil," *IEEE Trans. Signal Process.*, vol. 40, no. 9, pp. 2267-2280, Sep. 1992.
- [9] H. L. Van Trees, "Detection, Estimation, and Modulation Theory - Optimum Array Processing," (Part IV), Wiley, 2002.
- [10] D. Donoho, "Compressed sensing," *IEEE Trans. Inf. Theory.*, vol. 52, no. 4, pp. 1289-1306, Apr. 2006.
- [11] E. Candes, J. Romberg, and T. Tao, "Robust uncertainty principles: Exact signal reconstruction from highly incomplete frequency information," *IEEE Trans. Inf. Theory.*, vol. 52, no. 2, pp. 489-509, Feb. 2006.
- [12] M. Stojnic, " L_1 optimization and its various thresholds in compressed sensing," *ICASSP 2010*, pp. 3910-3913.
- [13] J. Tropp, "Just relax: Convex programming methods for identifying sparse signals in noise," *IEEE Trans. Inf. Theory.*, vol. 52, no. 3, pp. 1030-1051, 2006.
- [14] H. Zou, "The adaptive lasso and its oracle properties," *J. Amer. Statist. Assoc.*, vol. 101, no. 476, pp. 1418-1429, 2006.
- [15] J. A. Tropp, "Greed is good: Algorithmic results for sparse approximation," *IEEE Trans. Inf. Theory.*, vol. 50, no. 10, pp. 2231-2242, 2004.
- [16] D. Ramasamy, S. Venkateswaran, U. Madhow, "Compressive parameter estimation in AWGN," *IEEE Trans. Signal Process.*, vol. 62, no. 8, pp. 2012-2027, Apr. 2014.
- [17] Y. Chi, L. L. Scharf, A. Pezeshki, R. Calderbank, "Sensitivity to basis mismatch in compressed sensing," *IEEE Trans. Signal Process.*, vol. 59, no. 5, pp. 2182-2195, May. 2011.
- [18] A. Fannjiang, H.-C. Tseng, "Compressive radar with off-grid targets: A perturbation approach," *Inverse Problems*, vol. 29, no. 5, pp. 054008, 2013.
- [19] Z. Tan, P. Yang, A. Nehorai, "Joint sparse recovery method for compressed sensing with structured dictionary mismatch," *IEEE Trans. Signal Process.*, vol. 62, no. 19, pp. 4997-5008, Oct. 2014.
- [20] G. Tang, B. Bhaskar, P. Shah, B. Recht, "Compressed sensing off the grid," *IEEE Trans. Inf. Theory.*, vol. 59, no. 11, pp. 7465-7490, 2013.
- [21] N. I. Ahiezer, Mark Grigorevich Krein, "Some Questions in the Theory of Moments," *Translations of Mathematical Monographs, American Mathematical Society*. 1985.
- [22] C. Carathodory and L. Fejr, "Uber den Zusammenhang der extemen von harmonischen funktionen mit ihren koeffizienten und uber den Picard-Landauschen satz," *Rendiconti del Circolo Matematico diPalermo*, vol. 32, pp. 218-239, 1911.
- [23] Badri Narayan Bhaskar, Gongguo Tang, and Benjamin Recht, "Atomic norm denoising with applications to line spectral estimation," *IEEE Trans. Signal Process.*, vol. 61, no. 23, pp. 5987-5999, 2013.
- [24] Emmanuel J Candes and Carlos Fernandez-Granda, "Towards a mathematical theory of super-resolution," *Communications on Pure and Applied Mathematics.*, vol. 67, no. 6, pp. 906-956, 2014.
- [25] Y. Chi, Y. Chen, "Compressive two-dimensional harmonic retrieval via atomic norm minimization," *IEEE Trans. Signal Process.*, vol. 63, no. 4, pp. 1030-1042, Feb. 2015.
- [26] Zai Yang, Lihua Xie, and Petre Stoica, "Vandermonde decomposition of multilevel Toeplitz matrices with application to multidimensional super-resolution," *IEEE Transactions on Information Theory.*, vol. 62, no. 6, pp. 3685-3701, 2016.
- [27] E. Candes, J. Romberg, and T. Tao, "Robust uncertainty principles: Exact signal reconstruction from highly incomplete frequency information," *IEEE Trans. Inf. Theory.*, vol. 52, no. 2, pp. 489-509, Feb. 2006.
- [28] M. Grant and S. Boyd, "CVX: Matlab software for disciplined convex programming version 2.0 beta," [online] Available: <http://cvxr.com/cvx> Feb. 2015.
- [29] A. Schaeffer, "Inequalities of A. Markoff and S. Bernstein for polynomials and related functions," *Bull. Amer. Math. Soc.*, vol. 47, pp. 565-579, 1941.
- [30] R.P. Boas, JR, "Inequalities for the derivatives of polynomials," *Northwestern University, MATHEMATICS MAGAZINE*, Vol. 42, No. 4, September 1969.
- [31] Rockafellar, R. Tyrrell, "Convex Analysis," Princeton, *Princeton University Press*. (1997).
- [32] Kusraev A. G. and Kutateladze S. S, "Subdifferentials: theory and applications," *Mathematics and its Applications* Vol. 323, Kluwer Academic Publishers, Dordrecht, 1995.
- [33] B. Dumitrescu, "Positive Trigonometric Polynomials and Signal Processing Applications," New York, NY, USA: Springer, 2007.